

## Article

# The Statistical Analysis of Exoplanet and Host Stars Based on Multi-Satellite Data Observations

Yanke Tang<sup>1,2,\*,†</sup>, Xiaolu Li<sup>1</sup>, Kai Xiao<sup>3</sup>, Ning Gai<sup>1,\*,†</sup>, Shijie Li<sup>1</sup>, Futong Dong<sup>1</sup>, Yifan Wang<sup>1</sup>  
and Yang Gao<sup>1</sup>

<sup>1</sup> College of Physics and Electronic Information, Dezhou University, Dezhou 253023, China; lixiaolu@stu.dzu.edu.cn (X.L.); lishijie@dzu.edu.cn (S.L.); dongfutong@sohu.com (F.D.); nafiy@live.cn (Y.W.); gao14681@mail.ustc.edu.cn (Y.G.)

<sup>2</sup> Yunnan Key Laboratory, International Centre of Supernovae, Kunming 650216, China

<sup>3</sup> School of Astronomy and Space Science, University of Chinese Academy of Sciences, Beijing 100049, China; xiaokai@ucas.ac.cn

\* Correspondence: tyk@dzu.edu.cn (Y.T.); gaining@dzu.edu.cn (N.G.)

† These authors contributed equally to this work.

**Abstract:** In recent years, the rapid development of exoplanet research has provided us with an opportunity to better understand planetary systems in the universe and to search for signs of life. In order to further investigate the prevalence of habitable exoplanets and to validate planetary formation theories, as well as to comprehend planetary evolution, we have utilized confirmed exoplanet data obtained from the NASA Exoplanet Archive database, including data released by telescopes such as Kepler and TESS. By analyzing these data, we have selected a sample of planets around F, G, K, and M-type stars within a radius range of 1 to 20  $R_{\oplus}$  and with orbital periods ranging from 0.4 days to 400 days. Using the IDEM method based on these data, we calculated the overall formation rate, which is estimated to be 2.02%. Then, we use these data to analyze the relationship among planet formation rates, stellar metallicity, and stellar gravitational acceleration ( $\log g$ ). We firstly find that the formation rate of giant planets is higher around metal-rich stars, but it inhibits the formation of gas giants when  $\log g > 4.5$ , yet the stellar metallicity seems to have no effect on the formation rate of smaller planets. Secondly, the host stellar gravitational acceleration affects the relationship between planet formation rate and orbital period. Thirdly, there is a robust power-law relationship between the orbital period of smaller planets and their formation rate. Finally, we find that, for a given orbital period, there is a positive correlation between the planet formation rate and the  $\log g$ .

**Keywords:** planet; transiting exoplanets; planet formation rate; planet classification; giant planets; minor planets



**Citation:** Tang, Y.; Li, X.; Xiao, K.; Gai, N.; Li, S.; Dong, F.; Wang, Y.; Gao, Y. The Statistical Analysis of Exoplanet and Host Stars Based on Multi-Satellite Data Observations. *Universe* **2024**, *10*, 182. <https://doi.org/10.3390/universe10040182>

Academic Editor: Ana Inés Gómez de Castro

Received: 11 February 2024

Revised: 23 March 2024

Accepted: 7 April 2024

Published: 16 April 2024



**Copyright:** © 2024 by the authors. Licensee MDPI, Basel, Switzerland. This article is an open access article distributed under the terms and conditions of the Creative Commons Attribution (CC BY) license (<https://creativecommons.org/licenses/by/4.0/>).

## 1. Introduction

The discovery of thousands of transiting exoplanets via large-scale surveys, such as Kepler [1], K2 [2], and TESS [3], has enabled us to explore not only individual planets and systems but also planet populations. The current focal point of research in planetary formation theory centers on the study of protoplanetary disks and planetary embryos, as exemplified by contemporary concepts such as Pebble Accretion and Planetesimal Accretion. In traditional models of planetary formation, the growth of planetary embryos predominantly depends on binary collisions and coalescence. However, Pebble Accretion introduces a novel paradigm to our understanding. In circumstellar disks, planet formation starts with small dust, which slowly grows into pebbles, then condenses into planetesimals, and eventually forms larger planetary embryos through collisions [4–6]. When the mass of the planet's core is large enough, it will capture the gas from the accretion disk, and a planet is formed [7]. Pebble accretion is considered particularly crucial in the formation of terrestrial planet cores as well as the solid cores of giant planets. This mechanism also

elucidates the reasons for giant planet formation and carries significant implications for understanding the formation of giant planets and the early evolutionary dynamics of planetary systems. Planetesimal accretion, on the other hand, refers to the collisional accretion of planetesimals, which subsequently grow into planetary embryos, potentially culminating in the formation of the solid cores of terrestrial planets or giant planets. This highlights the complexity inherent in planetary formation. In this paper, we primarily investigate the element of planetary formation rates. Recent studies have discovered that stars of stellar type M are more conducive to the formation of Earth-like planets and super-Earths [8], while giant planets are rare [9,10]; it is estimated that about  $6.5 \pm 3.0\%$  of M dwarfs have a giant planet with a mass between 1 and  $13 M_j$ . In this work, we have found that planet formation rates are higher for stars of types G and K. Aside from this factor, stellar gravitational acceleration is also one of the influences on the planet formation rate, where stellar gravitational acceleration is related to stellar gravity. Protoplanetary disks, primarily composed of gases and dust, are subject to the motion effects caused by a star's gravity, which in turn impacts the evolutionary process of the disk. If the stellar gravitational acceleration is too high, it becomes challenging for the materials in the protoplanetary disk to coalesce, particularly in the case of giant planet formation. Although the occurrence of giant planets has been found to increase with stellar mass [11,12], the trend is the opposite for small planets. In our analysis, we also introduce the parameter of stellar gravitational acceleration for our focused investigation. Beyond these two factors, the metallicity of a star also affects the rate of planet formation. In existing research, on one hand, a correlation between giant planets and metallicity has been well established [13,14] and provides the key evidence for the core accretion model of planet formation [15,16]. On the other hand, such a planet-metallicity correlation is generally weaker and more complicated for small planets [17–20]. In this study, we have also engaged in a corresponding discussion on this topic.

In this paper, we analyze the planetary spawn rate using confirmed exoplanet data downloaded from NASA's exoplanet archive. A detailed introduction of the stars and planets within the dataset was conducted, and the planets were categorized using existing planetary classification models. Subsequently, we employed the inverse detection efficiency method to estimate the overall sample. Finally, we focused our research discussion on the impacts of the planetary orbital period, stellar metallicity, and stellar gravitational acceleration on the formation rate. This work has provided profound insights into our understanding of planetary formation and evolutionary theories and will aid future discoveries and classifications of small and giant planet populations, enhancing our deep comprehension of the mechanisms behind planet formation.

## 2. Data

As of 10 August 2023, the total number of confirmed exoplanets detected and released by various telescopes amounts to 5496<sup>1</sup>. Among them, there are 4096 planetary systems and a total of 1235 confirmed stellar spectra. Among the confirmed stellar spectra, there are 143 F-type stars, 329 G-type stars, 311 K-type stars, and 261 M-type stars. These data illustrate the ubiquitous existence of exoplanets in the universe and underscore the feasibility of exoplanet detection projects.

### 2.1. The Host Star

Based on these data, we have created a graphical representation of the effective temperatures ( $T_{eff}$ ) of the host star in relation to their gravitational ( $\log g$ ) acceleration in order to visually discern the distribution of stellar types within the selected data set, which are shown in Figure 1. From Figure 1, we find that there is a predominance of main sequence stars, with some red giants present. The color of the data points is represented by the Fe/H values, with darker colors indicating lower metal abundance in the main stars of the sample.

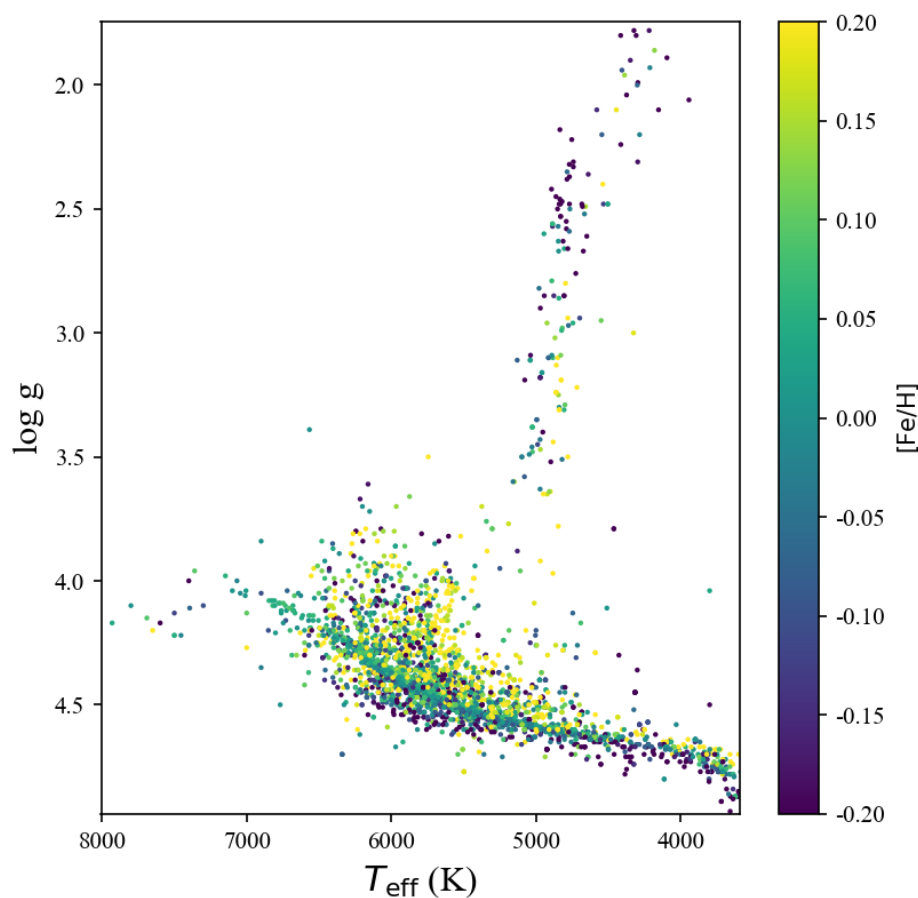


**Figure 1.** Distribution of host stars.

## 2.2. The Exoplanet

Having established the classification of stars within the dataset, we subsequently conducted a statistical analysis of the planetary constituents contained therein. Given that the search for suitable exoplanets cannot be constrained solely by stellar factors, we expanded our scrutiny beyond the stellar classifications to encompass an examination of the planets documented in our data set. G-type stars are also known as yellow dwarfs, like the Sun, but if you are looking for exoplanets, we can not just consider this single factor. We should also consider factors, such as the effect of the stellar radiant flux on the planet, the radius of the planet, and the orbital period of the planet. We have depicted the period distribution and radius distribution of transiting exoplanets around F, G, K, and M-type host stars, which are shown in Figures 2 and 3, respectively, to roughly analyze the orbital distributions of planets. From Figures 2 and 3, we find that the orbital period is mainly concentrated in 4–10 days, while the number of 100–400 days is less, and only the number of planets in this cycle range is higher under the K and G stellar types. As for the planetary radius, in addition to the F-type, the planetary radius of the other three type stars is concentrated in 1–4  $R_{\oplus}$ . There are more than 90 planets whose radii are 8–20  $R_{\oplus}$ , and whose host stars are F-type and G-type.

As we know, the K-type stars are more suitable candidates than G-type stars. This is because the boundaries of the habitable zone are not static in time and space, shifting outward with the evolution of the stellar main sequence phase. K-type stars evolve more slowly along the main sequence, providing a relatively stable habitable zone for planets. Therefore, we have listed some of the K-type stellar sample data (as shown in Table 1).

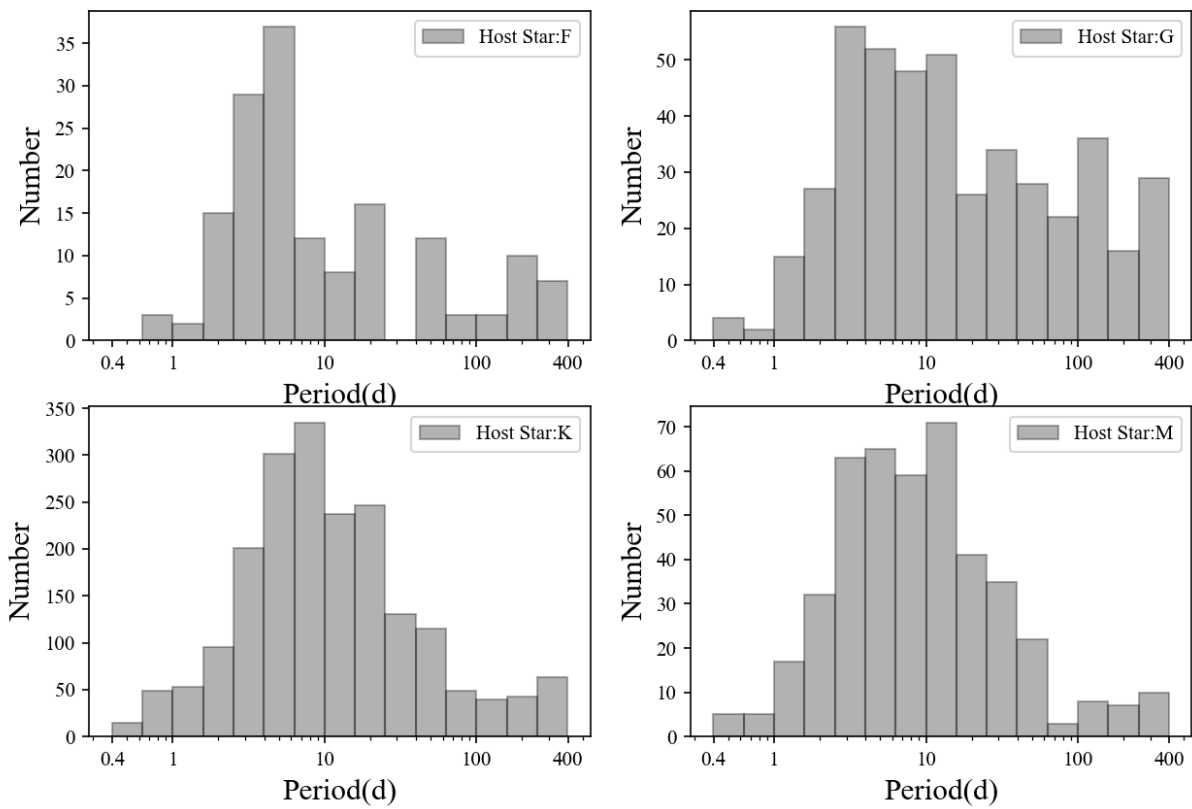


Figure 2. Period distribution of exoplanets whose host stellar are F, G, K, and M spectral types.

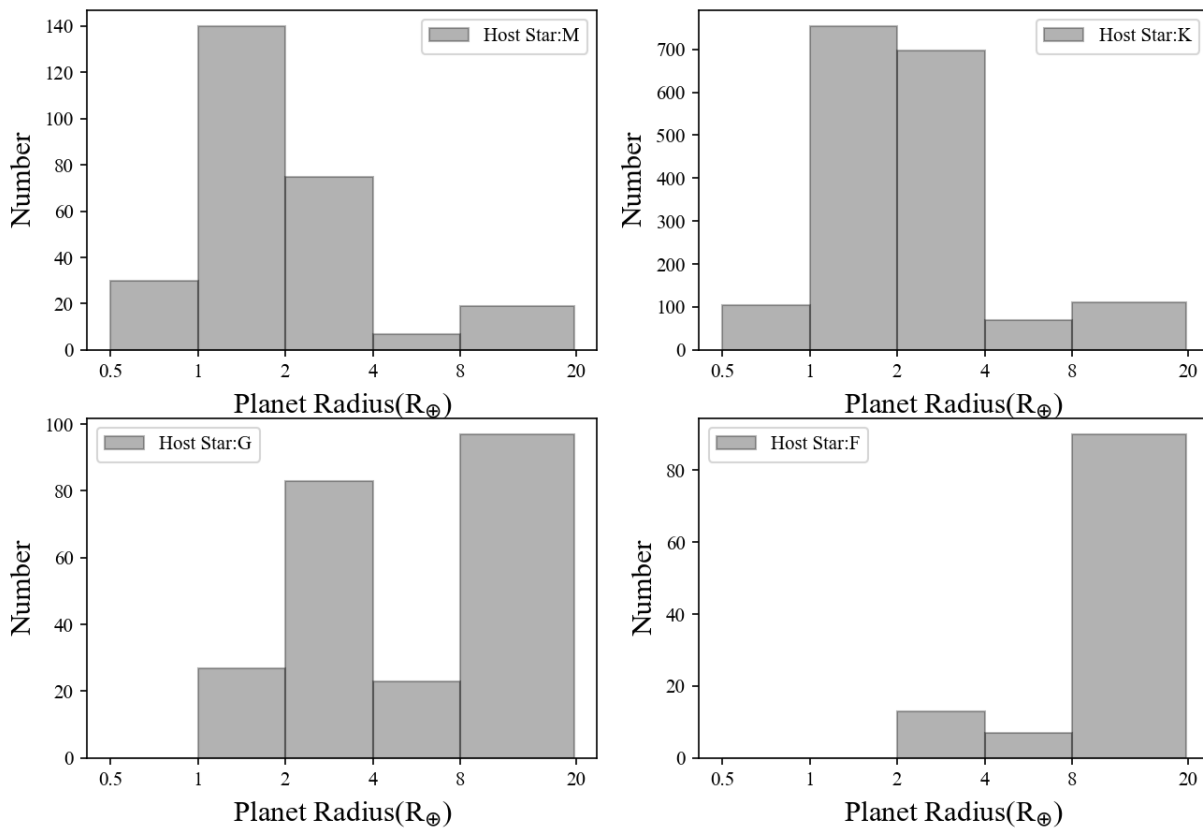


Figure 3. Radius distribution of exoplanets whose host stellars are F, G, K, and M spectral types.

**Table 1.** Catalog of high planet formation rates.

Planet Name	Period/d	Planet Radius/ $R_{\oplus}$	Stellar Type
CoRoT-24 b	5.1134	3.7	K1 V
EPIC 212737443 b	13.603	2.586	K3
EPIC 249893012 c	15.624	3.67	G8
HD 106315 b	9.55237	2.44	F5 V
HD 110082 b	10.18271	3.2	F8 V
HD 152843 b	11.6264	3.41	G0
HD 15337 c	17.1784	2.39	K1 V
HD 15906 b	10.924709	2.24	K V
HD 15906 c	21.583298	2.93	K V
HD 18599 b	4.1374354	2.6	K2 V
HD 191939 b	8.8803256	3.41	G9 V
HD 191939 c	28.579743	3.195	G9 V
HD 207496 b	6.441008	2.25	K2.5 V
HD 207897 b	16.202159	2.501	K0 V
HD 23472 b	17.667087	2	K4 V
HD 235088 b	7.4341393	2.045	K2 V
HD 28109 b	22.89104	2.199	F8/G0 V
HD 5278 b	14.339156	2.45	FV
HD 73583 b	6.39805	2.49	K4 V
HD 73583 c	18.87974	2.39	K4 V
HIP 94235 b	7.713057	3	G V
HIP 97166 b	10.28891	2.74	K0 V
K2-16 b	7.6188	2.02	K3 V
K2-16 c	19.07863	2.54	K3 V
K2-285 c	7.138048	3.53	K2 V
K2-285 d	10.45582	2.48	K2 V
Kepler-80 b	7.05246	2.67	K5
Kepler-80 c	9.52355	2.74	K5
TOI-1062 b	4.11296	2.265	G9 V
TOI-1130 b	4.066499	3.65	K7
TOI-1246 b	4.30744	3.01	K V
TOI-1246 c	5.904144	2.51	K V
TOI-1246 d	18.6559	3.51	K V
TOI-125 b	4.65382	2.726	K0 V
TOI-125 c	9.15059	2.759	K0 V

### 3. Planet Formation Rate (IDEM)

IDEM is a computationally efficient and effective method widely employed for the rapid estimation of the planet formation rate. IDEM facilitates a better understanding of the nature of planetary systems and allows for the estimation of the existence and properties of as-yet undetected planets. In the case of IDEM, we first need to specify the region data. Here, the data we use pertains to F, G, K, and M-type stars with radii ranging from 1 to 20  $R_{\oplus}$  and orbital periods ranging from 0.4 to 400 days. The planet formation rate within each grid, denoted as  $n_{cell}$ , is treated as a function correlated with the radius and orbital periods of the planets within the specified region. The number of planets is counted within each region from the data of various telescopes confirming the existence of exoplanets, with a subset of stars selected based on the sufficient precision of observations. Within the specified ranges of planetary radius and periods,  $n_{cell}$  is computed as:

$$n_{cell} = \sum_{j=1}^{N_{p,cell}} 1 / (N_{*,j} \times p_j) \quad (1)$$

where  $N_{p,cell}$  is the number of planetary samples within the specified region,  $p_j$  is the probability of planet  $j$  experiencing a transit event ( $1/p_j = a_j/R_*$ ),  $a_j$  represents the semi-

major axis of the planet, and  $R_*$  is the radius of the host stellar. All parameters in the formula can be obtained from the available data.

Although IDEM, as mentioned above, offers a rapid computational speed, it has limitations due to the lack of statistical theory support. Firstly, its estimations heavily rely on accurate assessments of detection efficiency. Any errors or inaccuracies in estimating the detection efficiency can consequently impact the results estimated by IDEM. Secondly, IDEM requires a substantial amount of observational data to obtain accurate estimations of detection efficiency. However, the current known quantity of exoplanets is relatively limited, leading to potential inaccuracies. Thirdly, IDEM typically necessitates assumptions and selections of parameters for the inverse model, and these choices can influence the estimation results. Inappropriate parameter assumptions may lead to inaccurate estimations. In summary, the inverse detection efficiency method is a useful statistical tool. However, to obtain more precise measurement results, it is advisable to incorporate the Bayesian framework for calculations.

According to the IDEM method, the overall distribution of the planet formation rate for F, G, K, and M-type stars is shown in Figure 4. For the selected range of planetary radii from 1 to 20  $R_{\oplus}$  and orbital periods from 0.4 to 400 days, the estimated planet formation rate around F, G, K, and M-type stars is 2.02%. The region with blank squares in Figure 4 represents a planet formation rate of 0. From Figure 4, we can visually observe that the planet formation rate is high for planets with radii ranging from 2 to 4  $R_{\oplus}$  and orbital periods ranging from 10 to 100 days, indicating a higher rate of formation for planets located in the inner orbits. Conversely, the planet formation rate is lower for orbits farther from the host star. These results are likely associated with the core accretion model and disk instability model mentioned earlier.

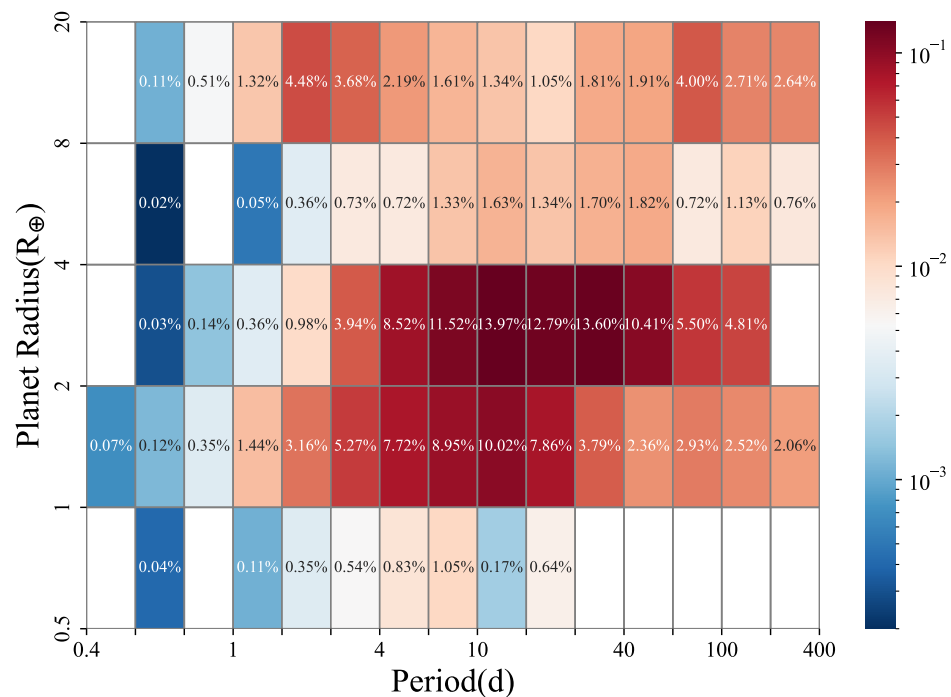


Figure 4. Distribution of overall formation rates estimated by IDEM around F, G, K, and M-type stars.

In addition, we listed the samples with the highest planet formation rate in the orbital period of 4–30 days, and the radius of the planets in the range of 2–4 $R_{\oplus}$ , and found that their host stars are basically G and K type, which is shown in Table 1.

After investigating the planet formation rate within the comprehensive sample data, we questioned whether the physical and chemical characteristics of different planetary types exerted an influence on their rates of formation. Consequently, we categorized the planetary samples in the dataset to facilitate further discussion on this matter.

#### 4. Planet Classification

Presently, the astronomical community has constructed a reasonable and reliable classification system for the classification of stars and galaxies, such as the Hertzsprung–Russell diagram and the Hubble Tuning Forks. Planet classification is crucial for a profound understanding of celestial bodies. Planet classification can assist in a better understanding of the diversity of planetary systems. Common classification criteria include the classification based on orbital position, physical properties, mass, orbital characteristics, and chemical features, among others. However, to obtain accurate classification results, multiple classification criteria should be considered simultaneously.

Regarding the current progress in planet classification, it can be divided into single-parameter classification, multi-parameter classification, and habitability classification. Single-parameter classification involves categorizing planets based on their mass. In the classification of mass, Michael<sup>2</sup> found values ranging from  $1.90 \times 10^{24}$  kg to  $1.90 \times 10^{30}$  kg [21]. Multi-parameter classification, building on mass differentiation, incorporates compositional classification. Stern and Levison [22] classify planets by mass into sub-dwarfs, dwarfs, sub-giants, giants, and supergiants. They further categorize planets based on composition, primarily focusing on rock, ice, and hydrogen. The final determination of a planet's type is based on its mass and composition. Habitability classification, such as the PHL's habitability classification, not only considers whether a planet is habitable but also categorizes habitable planets into sub-Earth-sized, Earth-sized, and super-Earth-sized types. Even within habitable terrestrial planets, further classification is necessary, particularly as slight variations in the abundance of certain elements can significantly impact habitable conditions [23]. For instance, concerning metallicity, stars with low metallicity have higher luminosity and effective temperature compared to stars of the same mass but with high metallicity [24], which subsequently affects the temperature of surrounding planets and the range of the habitable zone. Based on the data of confirmed exoplanets released by the NASA Exoplanet Archive, we conducted a simple planet classification according to a single parameter, as shown in Figure 5. As can be seen from this, in the data we analyzed, the number of super-Earths and giant planets is the largest, while the number of terrestrial planets is very rare.

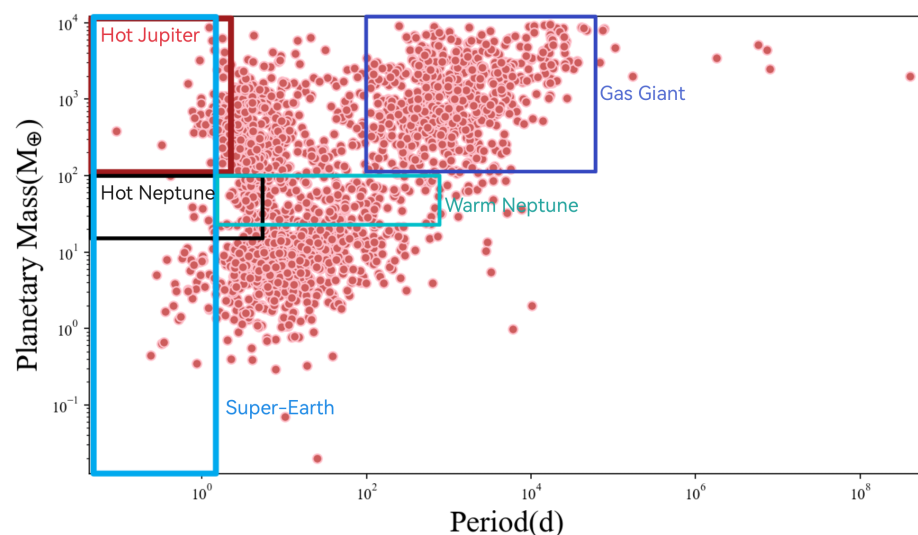


**Figure 5.** Planetary classification based on a single parameter.

For planet classification, there remain several shortcomings. Firstly, primarily based on physical features, most planet classifications are carried out through the physical characteristics of the planets. However, such classifications overlook factors like the planet's chemical composition and atmospheric conditions, which can significantly impact the properties and habitability of a planet. Habitability requires consideration of many conditions,

such as atmospheric composition, Earth similarity, and Earth temperature. Concerning Earth's temperature, the stellar radiation flux plays a vital role, and the distance between the planet and the stellar, along with the stellar temperature, determines this factor. Additionally, the stellar radiation flux is also related to a planet's habitability, atmospheric effects, and radiation type. Secondly, the lack of consideration for a planet's evolutionary history is crucial. The dynamic evolution of the galaxy and the evolution of planets are both significant factors. Thirdly, a limited number of classification parameters make it challenging to explain the diversity of planets in the universe. With so many unknown celestial bodies in the universe, the survey results of exoplanets only represent a fraction of what is out there. We cannot fully comprehend the various state models of planetary systems. These uncertainties and unknown factors prevent the planet classification models from reaching completeness.

Based on the above classification, for the convenience of our research, we can roughly divide planets into two categories, namely, giant planets and minor planets.

#### 4.1. Giant Planet

##### 4.1.1. Stellar Metallicity and The Planet Formation Rate

Early studies on the formation rate of giant planets were primarily conducted through radius velocity detection projects and the Kepler space telescope. The planet formation rate of giant planets with orbital periods shorter than a few years around solar-like stars is approximately 0.10, as Cumming et al. [25] suggested that the planet formation rate of giant planets with masses in the range of  $0.3\text{--}10 M_{Jup}$  ( $M_{Jup}$  is a Jupiter mass) and orbital periods ranging from 2 to 2000 days around solar-like stars is approximately 0.105. In the exoplanet statistics from Kepler, the planet formation rate for planets with a radius between 1 and  $20 R_{\oplus}$  and orbital periods between 0.5 and 400 days around F, G, K, and M-type stars is estimated to be  $0.23 \pm 0.06$  [26], while the formation rate for giant gas planets is estimated to be  $0.16 \pm 0.015$  [27]. In the context of the core accretion theory, heavy elements are essential for the formation of dust particles and minor planets that constitute the core of a planet. Consequently, protoplanetary disks rich in metals exhibit a higher surface density of solid materials, facilitating the more effective formation of rocky cores for gas giant planets [28]. Extensive research indicates that metal-rich stars are more likely to host neighboring giant planets, and the occurrence rate of such neighboring giant planets increases with the enhancement of metallicity [29]. So we observe the correlation between the metallicity and formation rate of giant planets but we did not find a conspicuous direct proportionality between the two variables in this question. Therefore, we hypothesize that there are other factors influencing the relationship between the two variables, leading us to introduce stellar surface gravity as an additional factor. This raises an issue that merits further discussion. According to the literature [14,19,20], the relevant formula for neighboring giant planets is as follows:

$$f(Z) = A(Z/Z_{\odot})^2 \quad (2)$$

where  $A$  is a normalization constant and  $A = 0.1369$  [19],  $f(Z)$  is the giant planet formation rate, and  $Z$  is stellar metallicity.

In response to the aforementioned hypothesis, we incorporated the variable of stellar surface gravity, quantified as  $\log g$ , and ultimately observed that  $\log g$  exerts a certain influence on the relationship between the two primary variables. Subsequently, we plotted the trends of their relationship across different  $\log g$  ranges. For this purpose, we chose the demarcation points for  $\log g$  at 2 and 3.5, and then performed a fitting analysis on the relationship between stellar metallicity and planet formation rate in each of the three intervals as depicted in the right panel of Figure 6. Our findings indicate that for stars with  $\log g < 2$  and  $\log g > 3.5$ , the trend lines appear relatively flat, differing in that the former shows a positive trend while the latter exhibits a negative one. In the intermediate range of  $2 < \log g < 3.5$ , we observe a much steeper slope, suggesting a more pronounced trend, and indicating that within this interval,  $\log g$  significantly influences the relationship

under consideration. This implies that in dwarf stars, the value of stellar metallicity has a minimal impact on the planet formation rate. To account for the significant discrepancy in the slopes, we propose the following speculations: Firstly, the mass of a star determines the gravitational acceleration within the circumstellar planet-forming disk; an increase in gravitational acceleration may enhance the density within the disk and the aggregation of material, thereby promoting the formation of planetary cores and, subsequently, giant planets. Secondly, if the stellar surface gravity is too strong, which is particularly evident in the case of giant planets, they form through a process known as the “core accretion model”, where a solid core forms first, and then starts to accrete surrounding gas through its gravity. An excessively high gravitational acceleration in the surrounding environment could inhibit the gas from converging towards this core, thus suppressing or delaying the formation of giant planets. Thirdly, an excessively high stellar surface gravity may also lead to material migrating too swiftly, thereby inhibiting the formation of planetary embryos. The failure to form a stable protoplanetary disk could naturally result in a reduced planet formation rate. This is also the reason why a negative trend is observed for  $\log g > 3.5$ .

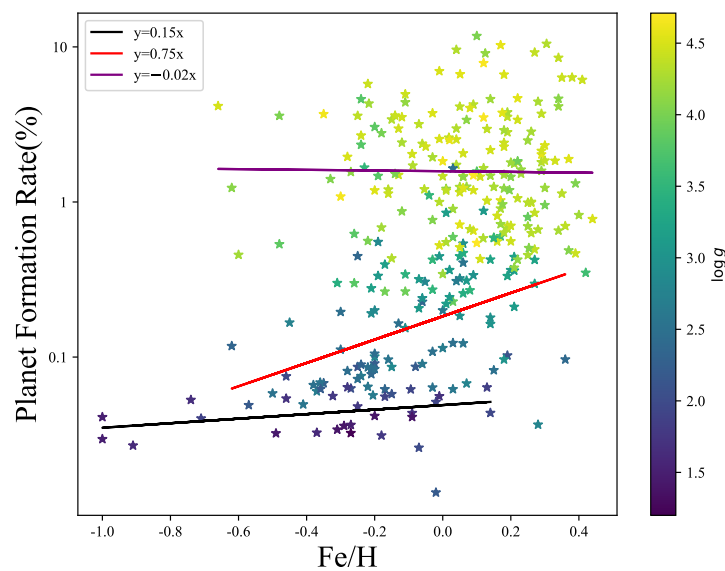


**Figure 6.** The correlation between stellar metallicity and the formation rate of giant planets.

#### 4.1.2. Orbital Period on the Formation Rates of Planets

According to the core accretion model, the formation process of planets necessitates the accumulation of matter, after which the accretion of the surrounding gas occurs. If a planet is located at a greater distance from its star, the lower density of matter can slow down the accumulation process, hence prolonging the time required to form a planet. In contrast, within the shorter-period inner regions, where matter is more concentrated, planets can form more quickly [30,31]. This phenomenon is one of the reasons why the orbital period affects the planet formation rate. To investigate this theory, we have conducted more detailed research.

We generated a scatter plot correlating the orbital periods of giant planets first. However, we did not yield satisfactory results, prompting an investigation into the underlying causes of this anomaly. Our initial hypothesis was that the spectral type of the host star might be influencing the correlation, but subsequent graphical analysis discounted this variable. Ultimately, we attributed the observed discrepancy to the gravitational ( $\log g$ ) acceleration of the host star.

This may be due to the fact that the gravitational acceleration of the host star can impact the distribution of matter density, temperature, and the dynamical processes within the surrounding disk, thereby affecting the planet formation rate and the final positioning of the formed planet. For instance, a greater gravitational acceleration might indicate that

the protoplanetary disk is more tightly held together, leading to a faster accumulation of material near the stellar body, which in turn accelerates the nucleation rate of the planets. Moreover, the gravitational field of the star can also affect the temperature structure of the protoplanetary disk, which in turn influences the growth rate of planetary embryos.

Therefore, we adjusted the color of the sample points to correspond with the magnitude of variations in  $\log g$  values to more distinctly observe the effect of  $\log g$  on their relationship. Following this, we generated a scatter plot incorporating two-dimensional variables (in the left panel of Figure 7), which allowed us to preliminarily ascertain that  $\log g$  values indeed influence the relationship, as it is evident that different segments of  $\log g$  values are located in varying regions of the figure. Consequently, when performing a linear fit, we introduced two-dimensional variables, namely the orbital period and  $\log g$ . We divided the fit into  $\log g$  intervals, creating separate fitting lines for when  $\log g$  equals 1, 2, 3, 4, and 5. From the figure, it is observable that the regression lines obtained for different  $\log g$  values have the same coefficients for both variables; the sole difference is in the intercepts. The overall fitting formula derived (as indicated in the left panel of Figure 7) is:

$$y = 0.68x_1 + 0.52x_2 - 4.05 \tag{3}$$

where  $x_1$  is the period, and  $x_2$  is  $\log g$ .

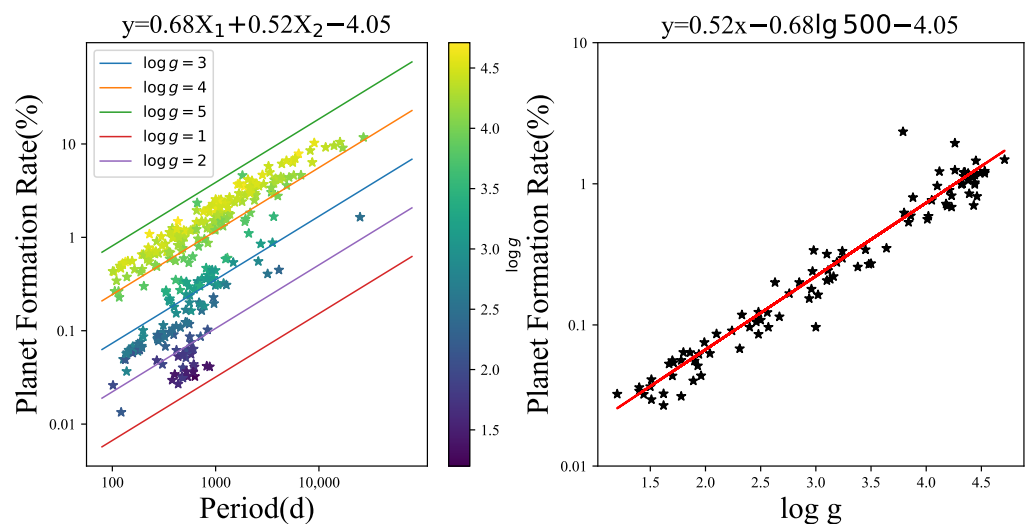


**Figure 7.** The relationship between the orbital periods of giant planets and the gravitational and formation rates.

For the orbital period and planet formation rate, we discovered a slope of 0.68, which is quite proximate to the planetary generation rate of  $2 \div 3$  observed in the solar system. This similarity allows us to speculate whether the formation principles of these systems mirror that of our own solar system. The implications of this resemblance are substantial in our search for suitable habitable exoplanets. Furthermore, it prompts an inquiry into whether there is a positive correlation between the stellar gravitational acceleration and the planet formation rate for planets with identical periods.

To substantiate this theory, we selected the sample interval with the highest number of samples, specifically from 300 d to 400 d, and then took the median value of 500 d to conduct a fit using the fitting formula calculated in the left panel of Figure 7. We found that the resulting fit perfectly matched the trend of the sample points within the chosen sample interval, which indirectly corroborates the validity of the theory in question, that is, for planets with identical periods, their formation rate is positively correlated with the gravitational ( $\log g$ ) acceleration of their host star (as shown in the right panel of Figure 7).

## 4.2. Minor Planets

Following the examination of the influence of giant planet characteristics on their formation rates, we also discussed the impact of asteroid metallicities and orbital periods on the planet formation rate.

### 4.2.1. Stellar Metallicity and the Planet Formation Rate

Minor planets are typically defined as planets with masses less than  $100 M_{\oplus}$  and orbital periods less than 100 days, such as Terrestrial Planets, Sub-Neptunes, and Warm Neptunes. Research on detections suggests a remarkably high formation rate for asteroids. This finding has propelled the emergence of new theories of planet formation, suggesting that low-mass planets can form directly in their original orbits, rather than forming initially in distant orbits and subsequently migrating to closer orbits. For minor planets, their formation rate shows a relatively weak correlation with the metallicity of the host star [17,19,32]. Therefore, we have also plotted the correlation scatter plot between the metallicity and formation rate of minor planets (as shown in Figure 8). In this figure, we have employed the same methodology as in Figure 6 to fit a scatter plot of the minor planets' formation rate to the metallicity of their host stars, incorporating the  $\log g$  parameter as a color code. However, unlike the case with giant planets, we do not observe any apparent correlation between the formation rate of minor planets and the metallicity of their host stars; alternatively, the minor planets' formation rate in correlation with the host star's metallicity appears to be more complex. Overall, the sample indicates a collective trend toward decline; in other words, a generation rate distribution above 0.5 can be observed at lower metallicities, while no sample points exhibit a generation rate exceeding 0.1 in metal-rich environments. Under these circumstances, the generation rate of minor planets is seemingly reduced. The distribution of the sample points is quite scattered, and the distribution of  $\log g$  is rather disordered. It is noteworthy, though, that the  $\log g$  values for minor planets are comparatively higher than those for giant planets, predominantly above 4.2, with the minimum reaching 3.4. In contrast, for giant planets, the lowest  $\log g$  is around 1.5 with a more substantial distribution. Can we consequently hypothesize that stars of the dwarf class are more conducive to the formation of asteroids, whereas giant stars are more likely to form giant planets? The specifics of this require further investigation with more detailed parameters, considering that the formation of planets is a complex cosmic phenomenon that is influenced by numerous factors.

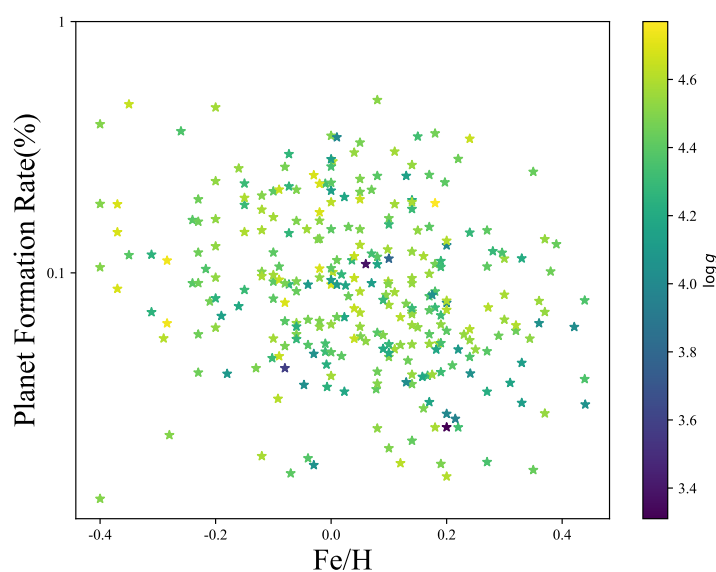


**Figure 8.** The correlation between stellar metallicity and the formation rate of minor planets.

We have now concluded our discussion on the relationship between stellar metallicity and planet formation rates. The rate of giant planet formation is regulated by the stellar metallicity, which explains why the early population of temperate terrestrial planets is more abundant than that of gas giants [29]. Overall, the planet formation rate not only depends on stellar properties such as spectral type and metallicity but also, on a larger scale in the Milky Way, these may not even be the primary factors influencing the planet formation rate. The specific reasons are attributed to the stellar dynamical history, understanding the stellar age and velocity, and its relationship with the distribution of planets. In a more recent work [33], it was found that stars with lower iron content and higher total velocities have a higher planet formation rate for near super-Earths and sub-Neptunes (with a radius ranging from 1–4  $R_{\oplus}$  and orbital periods less than 100 days). Therefore, the process of studying the planet formation rate remains long and challenging. Next, following the same methodology employed in our discussion of giant planets, we conducted a related research discussion on the relationship between the orbital period and formation rates of minor planets.

#### 4.2.2. Orbital Period on the Formation Rates of Planets

From the broad perspectives of cosmology and astrophysics, the orbital period of minor planets and their formation rates are two independent concepts and are generally not closely related. Observations made by plotting a minor planet’s orbital period against its formation rate have revealed a fascinating phenomenon (as shown in Figure 9). The resulting image diverges significantly from that of giant planets, with minor planets exhibiting a perfect power-law relationship and the sample distribution being relatively clustered. This suggests that these two variables are no longer independent; rather, they may be interconnected under specific environmental or conditional circumstances. For instance, minor planet orbits may be located in resonant regions, which are associated with the gravitational field of the host star. The confirmation of this power-law relationship can provide a profound understanding of the theories behind planetary formation and evolution. It also holds the potential to predict the behavior of other minor planet groups that have yet to be observed.

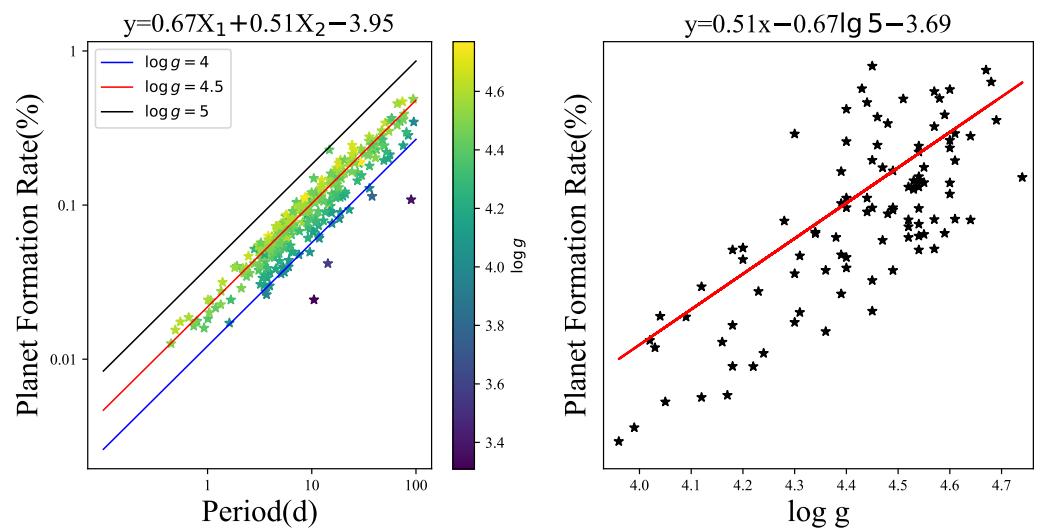


**Figure 9.** The relationship between the orbital periods of minor planets and formation rates and the relationship between the gravitational and their formation rates.

To ensure the rigor of our conclusions, we have reintroduced the  $\log g$  parameter (the left of Figure 9), ultimately finding that its impact on the relationship between asteroid orbital periods and formation rates is analogous to that observed for giant planets. As with the scenarios presented in Figure 7, differing  $\log g$  values are distributed across distinct regions. We have categorized these distributions into two intervals:  $4 < \log g < 4.5$  and  $4.5 < \log g < 5$ . Subsequently, in our curve-fitting process, we incorporated a two-

dimensional variable, namely  $\log g$  and orbital period. The fitting formula that we derived (also depicted on the left of Figure 9) is as follows:

$$y = 0.67x_1 + 0.51x_2 - 3.95 \tag{4}$$

where  $x_1$  is period, and  $x_2$  is  $\log g$ .

From the formula, it is observed that the slope of the relationship between the orbital period and formation rate is 0.67, which is in complete agreement with that of our solar system. This concurrence is of substantial significance for the advancement of planetary formation theories.

Similarly, we have also generated a plot illustrating the relationship between  $\log g$  and the formation rate at prime orbital periods (as shown in the right of Figure 9). We selected the sample interval with the highest number of samples, specifically between 3 d and 7 d, and then took the median value of 5 d. Utilizing the fitting formula calculated from the left panel of Figure 9, we conducted a fit, and the results remain in perfect agreement, further substantiating the positive correlation between the formation rates of asteroids and the gravitational acceleration of their host stars ( $\log g$ ) at constant orbital periods.

#### 4.2.3. The Mass and Radius

In the study of small planet data, we have also made an interesting discovery [34], namely, that the mass of a minor planet is roughly proportional to the planet’s radius (as shown in Figure 10). If the minor planet is treated as a spheroid and fits the density formula, this finding indicates that the density of the minor planet tends to a certain value, it also means that the planet is proportional to the radius squared. However, this proportional relationship does not hold for giant planets. To draw more reliable conclusions, we included asteroids within the solar system for reference. Unsurprisingly, asteroids in the solar system also followed the trend of positive correlation, which is undoubtedly a good result. However, due to the differences between the solar system and the planetary systems in our selected samples as well as observational errors, the fitting line we obtained is not very close to the solar system data. Nevertheless, it can still generally explain the trend.

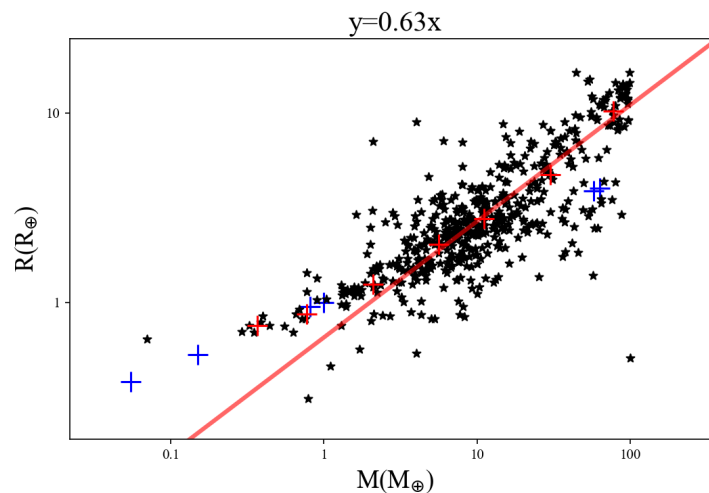


**Figure 10.** The correlation between the mass and radius of minor planets, the red plus sign indicates taking the bin and the blue plus sign indicates planets within the solar system.

### 5. Conclusions

Exoplanets have always been a popular research area in astronomy. Since the first discovery of exoplanets in the early 1990s, scientists have confirmed the existence of thousands of exoplanets. The study of exoplanets is of significant importance for understanding the formation and evolution of planetary systems, the search for habitable worlds, comprehending the context of the solar system, and exploring the diversity of life in the universe. Similarly, it also presents new directions for planetary research.

In this paper, we analyzed the data released by the NASA Exoplanet Archive and conducted a statistical analysis of the period distribution and radius distribution of exoplanets with host stars of spectral types F, G, K, and M. We found that the statistical analysis was conducted on the types of stars and planets, revealing that the majority of stars are dwarfs, specifically of G and K types. The number of exoplanets follows a roughly normal distribution in the orbital period range of 0.4 to 400 days, while the radius distribution is relatively irregular, with planets concentrating around  $1\text{--}4 R_{\oplus}$  and  $8\text{--}20 R_{\oplus}$ . We conducted an estimation of the overall population of exoplanets ranging from 0.4 to 400 days in orbital period and 1 to 20 Earth radii using the inverse detection efficiency method, resulting in an estimated value of 2.02. After analyzing the overall planet formation rate, we delved into a more detailed discussion of whether different types of stars exert the same influence on their formation rates. Therefore, we classified the exoplanets in the dataset into broad categories, following the existing planetary classification theoretical models, simplistically categorizing the sample into two groups: minor planets and giant planets. We focused on discussing the impact of host star metallicity and surface gravity, as well as planetary orbital periods on the formation rates of these two categories. Ultimately, we found that giant planets have a higher formation rate under rich metallicity conditions, while this factor is even more complex for minor planets. In addition, stellar gravity (measured as  $\log g$ ) modifies the relationship between giant planet formation rates and stellar metallicity, with lower  $\log g$  values correlating with consistently lower formation rates regardless of metallicity, and higher  $\log g$  values correlating with generally higher formation rates. Consequently, we hypothesize that an excessively high gravitational acceleration of a star may inhibit the formation of giant planets, while an excessively low acceleration may affect the rate of giant planet formation, thereby influencing the speed at which their protoplanetary disks are formed. Pertaining to orbital periods, small planets exhibit a distinct power-law relationship with their formation rates, whereas the proportional relationship for giant planets is less well-defined, which we identified as being influenced by stellar surface gravity. Similarly, stellar surface gravity affects the relationship between orbital periods and formation rates for small planets. This may be due to a wider distribution of metallicity values in giant planets, with sample points spread across various intervals and nearly equal distribution numbers, whereas metallicity values for stars hosting small planets are more densely clustered, resulting in a better fit. Moreover, we made an interesting observation about minor planets: their mass and radius display a power-law relationship, suggesting that the density of small planets tends toward a constant value. In this paper, we analyzed the data released by the NASA Exoplanet Archive and conducted a statistical analysis of the period distribution and radius distribution of exoplanets with host stars of spectral types F, G, K, and M. We found that the statistical analysis was conducted on the types of stars and planets, revealing that the majority of stars are dwarfs, specifically of G and K types. The number of exoplanets follows a roughly normal distribution in the orbital period range of 0.4 to 400 days, while the radius distribution is relatively irregular, with planets concentrating around  $1\text{--}4 R_{\oplus}$  and  $8\text{--}20 R_{\oplus}$ . We conducted an estimation of the overall population of exoplanets ranging from 0.4 to 400 days in orbital period and 1 to 20 Earth radii using the inverse detection efficiency method, resulting in an estimated value of 2.02%. After analyzing the overall planet formation rate, we delved into a more detailed discussion of whether different types of stars exert the same influence on their formation rates. Therefore, we classified the exoplanets in the dataset into broad categories, following the existing planetary classification theoretical models, simplistically categorizing the sample into two groups: minor planets and giant planets. We focused on discussing the impact of host star metallicity and surface gravity, as well as planetary orbital periods on the formation rates of these two categories. Ultimately, we found that giant planets have a higher formation rate under rich metallicity conditions, while this factor is even more complex for minor planets. In addition, stellar gravity (measured as  $\log g$ ) modifies the relationship between giant planet formation rates and stellar metallicity, with lower  $\log g$  values correlating with consistently lower formation rates regardless of metallicity,

and higher  $\log g$  values correlating with generally higher formation rates. Consequently, we hypothesize that an excessively high gravitational acceleration of a star may inhibit the formation of giant planets, while an excessively low acceleration may affect the rate of giant planet formation, thereby influencing the speed at which their protoplanetary disks are formed. Pertaining to orbital periods, small planets exhibit a distinct power-law relationship with their formation rates, whereas the proportional relationship for giant planets is less well-defined, which we identified as being influenced by stellar surface gravity. Similarly, stellar surface gravity affects the relationship between orbital periods and formation rates for small planets. This may be due to a wider distribution of metallicity values in giant planets, with sample points spread across various intervals and nearly equal distribution numbers, whereas metallicity values for stars hosting small planets are more densely clustered, resulting in a better fit. Moreover, we made an interesting observation about minor planets: their mass and radius display a power-law relationship, suggesting that the density of small planets tends toward a constant value.

In this paper, two points merit discussion. The first concerns the orbital period's coefficient value for both minor planets and giant planets, which is about 0.67, prompting us to question whether the formation of the sampled planets is akin to the accretion disk theory, as is supposed for our solar system. The second point is our observation that the metallicity of stars hosting small planets is generally higher, with most values exceeding 4.2 and the lowest around 3.4. Conversely, the metallicity of stars hosting giant planets has a minimum value of approximately 1.5, with a distribution of points that closely mirrors that of higher values. This raises the question of whether it might be more feasible for small planets to form around dwarf stars and giant planets around more massive stars. Further analysis, incorporating more parameters, is required to explore these findings in detail.

The study of habitable exoplanets, one of the most critical scientific questions, has so far only identified Earth as a habitable planet. In this paper, we focused more on analyzing the data of planets around solar-like stars. Due to our limited understanding of the universe, the determination of habitable zones can only be inferred based on the structure of the solar system, which is undoubtedly still in its nascent stage. However, the advancement of detection technology will expand our understanding of the universe, and various theories will continue to advance. The TESS satellite has taken over the task of the Kepler satellite, and future satellites with stronger observation capabilities and precision will be launched into space. We will continue to discover new exoplanets, gradually broaden our cosmic perspective, further refine planetary formation theories, and deepen our understanding of life.

**Author Contributions:** Conceptualization, Y.T. and N.G.; methodology, Y.T. and K.X.; software, X.L.; formal analysis, F.D. and X.L.; investigation, Y.G.; resources, Y.W.; data curation, S.L.; writing—original draft preparation, X.L.; writing—review and editing, Y.T.; funding acquisition, Y.T. All authors have read and agreed to the published version of the manuscript.

**Funding:** This research was funded by the National Natural Science Foundation of China (Grant No. U1931106), Shandong Provincial Natural Science Foundation of China (Grant Nos. ZR2019YQ03 and ZR2023MA036), and Project of Shandong QingChuang Science and Technology Plan (Grant No. 2019KJJ006). Yanke Tang is supported by the International Centre of Supernovae, Yunnan Key Laboratory (Nos. 202302AN360001 and 202302AN36000103).

**Data Availability Statement:** Data are contained within the article.

**Conflicts of Interest:** The authors declare no conflicts of interest.

## Notes

<sup>1</sup> <https://exoplanetarchive.ipac.caltech.edu/> (accessed on 10 August 2023).

<sup>2</sup> <http://rocketforge.org/2009/06/09/a-planetary-classification-proposal.html> (accessed on 10 August 2023).

## References

1. Borucki, W.J.; Koch, D.; Basri, G.; Batalha, N.; Brown, T.; Caldwell, D.; Caldwell, J.; Christensen-Dalsgaard, J.; Cochran, W.D.; DeVore, E.; et al. Kepler planet-detection mission: Introduction and first results. *Science* **2010**, *327*, 977–980. [[CrossRef](#)] [[PubMed](#)]
2. Howell, S.B.; Sobeck, C.; Haas, M.; Still, M.; Barclay, T.; Mullally, F.; Troeltzsch, J.; Aigrain, S.; Bryson, S.T.; Caldwell, D.; et al. The K2 mission: Characterization and early results. *Publ. Astron. Soc. Pac.* **2014**, *126*, 398. [[CrossRef](#)]
3. Ricker, G.R.; Winn, J.; Vanderspek, R.; Latham, D.; Bakos, G.; Bean, J.; Berta-Thompson, Z.; Brown, T.M.; Buchhave, L.; Butler, N.R.; et al. Transiting Exoplanet Survey Satellite. *J. Astron. Telesc. Instrum. Syst.* **2015**, *1*, 014003. [[CrossRef](#)]
4. Birnstiel, T.; Dullemond, C.P.; Brauer, F. Gas- and dust evolution in protoplanetary disks. *Astron. Astrophys.* **2010**, *513*, A79, [[CrossRef](#)]
5. Garaud, P.; Meru, F.; Galvagni, M.; Olczak, C. From Dust to Planetesimals: An Improved Model for Collisional Growth in Protoplanetary Disks. *Astrophys. J.* **2013**, *764*, 146, [[CrossRef](#)]
6. Kenyon, S.J.; Najita, J.R.; Bromley, B.C. Rocky Planet Formation: Quick and Neat. *Astrophys. J.* **2016**, *831*, 8, [[CrossRef](#)]
7. Morbidelli, A.; Lunine, J.; O'Brien, D.; Raymond, S.; Walsh, K. Building Terrestrial Planets. *Annu. Rev. Earth Planet. Sci.* **2012**, *40*, 251–275. [[CrossRef](#)]
8. Mulders, G.D.; Drażkowska, J.; van der Marel, N.; Ciesla, F.J.; Pascucci, I. Why Do M Dwarfs Have More Transiting Planets? *Astrophys. J. Lett.* **2021**, *920*, L1, [[CrossRef](#)]
9. Schlecker, M.; Burn, R.; Sabotta, S.; Seifert, A.; Henning, T.; Emsenhuber, A.; Mordasini, C.; Reffert, S.; Shan, Y.; Klahr, H. RV-detected planets around M dwarfs: Challenges for core accretion models. *Astron. Astrophys.* **2022**, *664*, A180, [[CrossRef](#)]
10. Montet, B.T.; Crepp, J.R.; Johnson, J.A.; Howard, A.W.; Marcy, G.W. The TRENDS High-contrast Imaging Survey. IV. The Occurrence Rate of Giant Planets around M Dwarfs. *Astrophys. J.* **2014**, *781*, 28, [[CrossRef](#)]
11. Johnson, J.A.; Aller, K.M.; Howard, A.W.; Crepp, J.R. Giant planet occurrence in the stellar mass-metallicity plane. *Publ. Astron. Soc. Pac.* **2010**, *122*, 905. [[CrossRef](#)]
12. Ghezzi, L.; Montet, B.T.; Johnson, J.A. Retired stars revisited: An updated giant planet occurrence rate as a function of stellar metallicity and mass. *Astrophys. J.* **2018**, *860*, 109. [[CrossRef](#)]
13. Santos, N.C.; Israelian, G.; Mayor, M. The metal-rich nature of stars with planets. *Astron. Astrophys.* **2001**, *373*, 1019–1031. [[CrossRef](#)]
14. Fischer, D.A.; Valenti, J. The planet-metallicity correlation. *Astrophys. J.* **2005**, *622*, 1102. [[CrossRef](#)]
15. Pollack, J.B.; Hubickyj, O.; Bodenheimer, P.; Lissauer, J.J.; Podolak, M.; Greenzweig, Y. Formation of the giant planets by concurrent accretion of solids and gas. *Icarus* **1996**, *124*, 62–85. [[CrossRef](#)]
16. Ida, S.; Lin, D.N. Toward a deterministic model of planetary formation. I. A desert in the mass and semimajor axis distributions of extrasolar planets. *Astrophys. J.* **2004**, *604*, 388. [[CrossRef](#)]
17. Buchhave, L.A.; Latham, D.W.; Johansen, A.; Bizzarro, M.; Torres, G.; Rowe, J.F.; Batalha, N.M.; Borucki, W.J.; Brugamyer, E.; Caldwell, C.; et al. An abundance of small exoplanets around stars with a wide range of metallicities. *Nature* **2012**, *486*, 375–377. [[CrossRef](#)] [[PubMed](#)]
18. Dong, S.; Xie, J.W.; Zhou, J.L.; Zheng, Z.; Luo, A. LAMOST telescope reveals that Neptunian cousins of hot Jupiters are mostly single offspring of stars that are rich in heavy elements. *Proc. Natl. Acad. Sci. USA* **2018**, *115*, 266–271. [[CrossRef](#)] [[PubMed](#)]
19. Petigura, E.A.; Marcy, G.W.; Winn, J.N.; Weiss, L.M.; Fulton, B.J.; Howard, A.W.; Sinukoff, E.; Isaacson, H.; Morton, T.D.; Johnson, J.A. The California-Kepler survey. IV. Metal-rich stars host a greater diversity of planets. *Astron. J.* **2018**, *155*, 89. [[CrossRef](#)]
20. Zhu, W. Influence of Stellar Metallicity on Occurrence Rates of Planets and Planetary Systems. *Astrophys. J.* **2019**, *873*, 8. [[CrossRef](#)]
21. Swedenborg, E. *Latin: Opera Philosophica et Mineralia* (English: Philosophical and Mineralogical Works). Principia, 1. 1973. Available online: <https://www.britannica.com/topic/Opera-Philosophica-et-Mineralia> (accessed on 17 July 2023).
22. Stern, S.A.; Levison, H.F. Regarding the criteria for planethood and proposed planetary classification schemes. *Highlights Astron.* **2002**, *12*, 205–213. [[CrossRef](#)]
23. Mayor, M.; Queloz, D. A Jupiter-mass companion to a solar-type star. *Nature* **1995**, *378*, 355–359. [[CrossRef](#)]
24. Tout, C.A.; Pols, O.R.; Eggleton, P.P.; Han, Z. Zero-age main-sequence radii and luminosities as analytic functions of mass and metallicity. *Mon. Not. R. Astron. Soc.* **1996**, *281*, 257–262. [[CrossRef](#)]
25. Cumming, A.; Butler, R.P.; Marcy, G.W.; Vogt, S.S.; Wright, J.T.; Fischer, D.A. The Keck planet search: Detectability and the minimum mass and orbital period distribution of extrasolar planets. *Publ. Astron. Soc. Pac.* **2008**, *120*, 531. [[CrossRef](#)]
26. Thompson, S.E.; Coughlin, J.L.; Hoffman, K.; Mullally, F.; Christiansen, J.L.; Burke, C.J.; Bryson, S.; Batalha, N.; Haas, M.R.; Catanzarite, J.; et al. Planetary candidates observed by Kepler. VIII. A fully automated catalog with measured completeness and reliability based on data release 25. *Astrophys. J. Suppl. Ser.* **2018**, *235*, 38. [[CrossRef](#)] [[PubMed](#)]
27. Zhu, W.; Dong, S. Exoplanet statistics and theoretical implications. *Annu. Rev. Astron. Astrophys.* **2021**, *59*, 291–336. [[CrossRef](#)]
28. Ida, S.; Lin, D. Toward a deterministic model of planetary formation. II. The formation and retention of gas giant planets around stars with a range of metallicities. *Astrophys. J.* **2004**, *616*, 567. [[CrossRef](#)]
29. Madau, P. Beyond the Drake Equation: A Time-dependent Inventory of Habitable Planets and Life-bearing Worlds in the Solar Neighborhood. *Astrophys. J.* **2023**, *957*, 66. [[CrossRef](#)]
30. Fortier, A.; Alibert, Y.; Carron, F.; Benz, W.; Dittkrist, K.M. Planet formation models: The interplay with the planetesimal disc. *Astron. Astrophys.* **2013**, *549*, A44. [[CrossRef](#)]

31. Mordasini, C.; Klahr, H.; Alibert, Y.; Benz, W.; Dittkrist, K.M. Theory of planet formation. *arXiv* **2010**, arXiv:1012.5281.
32. Sousa, S.; Santos, N.; Mayor, M.; Udry, S.; Casagrande, L.; Israelian, G.; Pepe, F.; Queloz, D.; Monteiro, M. Spectroscopic parameters for 451 stars in the HARPS-GTO planet search program—stellar [Fe/H] and the frequency of exo-Neptunes. *Astron. Astrophys.* **2008**, *487*, 373–381. [[CrossRef](#)]
33. Bashi, D.; Zucker, S. Small Planets in the Galactic Context: Host Star Kinematics, Iron, and Alpha-element Enhancement. *Astron. J.* **2019**, *158*, 61. [[CrossRef](#)]
34. Mousavi-Sadr, M.; Jassur, D.M.; Gozaliasl, G. Revisiting mass–radius relationships for exoplanet populations: A machine learning insight. *Mon. Not. R. Astron. Soc.* **2023**, *525*, 3469–3485. [[CrossRef](#)]

**Disclaimer/Publisher’s Note:** The statements, opinions and data contained in all publications are solely those of the individual author(s) and contributor(s) and not of MDPI and/or the editor(s). MDPI and/or the editor(s) disclaim responsibility for any injury to people or property resulting from any ideas, methods, instructions or products referred to in the content.